Published in final edited form as:
Exp Neurol. 2007 September ; 207(1): 42–51. doi:10.1016/j.expneurol.2007.05.023.

Escalating dose-multiple binge methamphetamine exposure results in degeneration of the neocortex and limbic system in the rat

Ronald Kuczenski[a], **Ian P Everall**[a], **Leslie Crews**[b], **Anthony Adame**[c], **Igor Grant**[c,d], and **Eliezer Masliah**[b,c,*]

[a] Department of Psychiatry, and the HIV Neurobehavioral Research Center, University of California, San Diego/La Jolla, CA, USA

[b] Department of Pathology, and the HIV Neurobehavioral Research Center, University of California, San Diego/La Jolla, CA, USA

[c] Department of Neurosciences, and the HIV Neurobehavioral Research Center, University of California, San Diego/La Jolla, CA, USA

[d]Veterans Affairs Healthcare System, La Jolla, CA USA

Abstract

Abuse of stimulant drugs such as methamphetamine (METH) and cocaine has been associated with long-lasting persistent behavioral alterations. Although METH-induced changes in the striatal dopaminergic system might play a role in these effects, the potential underlying neuroanatomical substrate for the chronic cognitive dysfunction in METH users is unclear. To investigate the involvement of non-dopaminergic systems in the neurotoxic effects of METH, we treated rats with an escalating dose-multiple binge regimen, which we have suggested may more closely simulate human METH exposure profiles. Combined neuropathological and stereological analyses showed that 30 days after the last binge, there was shrinkage and degeneration in the pyramidal cell layers of the frontal cortex and in the hippocampal CA3 region. Further immunocytochemical analysis showed that METH exposure resulted in loss of calbindin interneurons in the neocortex and selective damage to pyramidal neurons in the CA3 region of the hippocampus and granular cells in the dentate gyrus that was accompanied by microglial activation. Taken together, these studies suggest that selective degeneration of pyramidal neurons and interneurons in the neocortex and limbic system might be involved in the cognitive alterations in METH users.

Keywords

Calbindin immunoreactivity; hippocampus; pyramidal neurons; Methamphetamine

*Correspondence and reprint requests should be addressed to: Dr. E. Masliah, Department of Neurosciences, University of California San Diego, La Jolla, CA 92093-0624. Phone (858) 534-8992, Fax (858) 534-6232, e-mail: emasliah@ucsd.edu.

Introduction

Methamphetamine (METH) abuse has been associated with persistent behavioral changes and relatively long-lasting functional alterations (Kalechstein et al., 2003; London et al., 2004; Nordahl et al., 2003; Sim et al., 2002; Simon et al., 2002; Volkow et al., 2001b; Volkow et al., 2001c). Most efforts to study potential underlying neuroanatomical/neurochemical substrates have focused on dopamine (DA) systems, particularly striatal DA, because DA appears to play a critical role in the behavioral and reinforcing effects of METH-like stimulants (Creese and Iversen, 1974; Koob et al., 1998; Swerdlow et al., 1986; Wise and Rompre, 1989), and because striatal DA appears to be particularly susceptible to persistent alterations when exposed to high doses of this drug. In animal models, acute administration of high doses of METH results in decrements in markers of striatal DA nerve terminals (Maragos et al., 2002; Ricaurte et al., 1982; Ricaurte et al., 2002). Similarly, METH abusers also exhibit striatal DA decrements, and these alterations can persist for prolonged periods (McCann et al., 1998; Sekine et al., 2001; Volkow et al., 2001a). While the neurotoxic effects of METH in the nigral system might explain some of the behavioral and motor alterations, the anatomical bases for the cognitive disturbances in these patients are less well understood and suggest that other neuronal populations in the neocortex and limbic system might be affected by METH.

In support of this possibility, previous studies have shown that in addition to striatal DA, other non-striatal, non-DA systems are altered by exposure to METH. For example, early studies indicated that METH promoted persistent decrements in serotonin, particularly in the hippocampus (see, for example, (Ricaurte et al., 1980)), and more recently METH-induced damage to neurons in the somatosensory cortex has been characterized by TUNEL staining (Deng et al., 2001), and documented utilizing fluoro-Jade detection (Schmued and Bowyer, 1997) and other techniques (O'Dell and Marshall, 2000; Pu et al., 1996). Likewise, in human METH abusers, persistent alterations and structural abnormalities have been reported in brain regions receiving relatively sparse DA innervation (Volkow et al., 2001b). Moreover, recent studies have shown that in HIV patients with a history of METH abuse there is considerable damage to calbindin- immunoreactive interneurons in the neocortex and striatum (Langford et al., 2003) that is associated with the memory deficits in these patients (Chana et al., 2006). Taken together, these studies suggest that METH might damage other non-DA neuronal populations involved in cognitive function. However, very limited experimental data are currently available about neuronal populations affected in models of METH toxicity.

To further examine potential neuronal damage associated with METH exposure, we treated animals with an escalating dose-multiple binge (ED-MB) treatment regimen which we have suggested may more closely simulate human METH exposure profiles (Segal and Kuczenski, 1997; Segal et al., 2003), and combined neuropathological, stereological and immunocytochemical analyses were used to assess potential alterations. Our analyses revealed decrements in two unique populations of neurons in the neocortex and hippocampus.

Materials and methods

Animals

For these studies a total of 30 male Sprague-Dawley rats (Harlan Labs, San Diego, CA) weighing 325–350g at the beginning of drug treatment, were housed for at least one week prior to treatment in groups of two or three in wire mesh cages, with ad libitum access to food and water, in a temperature- and humidity-controlled room. The room was maintained on a reversed 12 h dark (0700–1900), 12 h light cycle to enable experimentation during the normal active phase of the awake/sleeping cycle. During the dark period, all facilities were illuminated with red light. To facilitate habituation to the procedures, animals were handled and injected with saline at least once per day. During the remainder of the day and night, animals were not

disturbed. Three days prior to initiation of drug administration, animals were housed individually.

Methamphetamine administration and tissue processing

D-Methamphetamine hydrochloride (Sigma-Aldrich, St. Louis, MO) was dissolved in saline and administered subcutaneously (s.c.); doses represent free base. Following the habituation period, groups of animals were initially exposed to the ED-phase of drug administration (starting with 0.1 mg/kg and escalating to 4.0 mg/kg). During this phase, animals received three injections, s.c., per day of saline or doses of METH that were gradually increased for 14d (Table 1). On the day following the ED-pretreatment, animals were exposed daily for 11 successive days to a high-dose METH binge, each binge consisting of four successive injections of 6.0 mg/kg METH at 2h intervals, beginning at 0900. During treatment, no animals showed symptoms of distress and minimal evidence of hyperthermia. Tolerance to these deleterious effects develops during the ED pretreatment prior to “binges.” In contrast, in most other high dose METH treatments, there is typically a moderate level of mortality. At 3 or 30 days (d) after the last binge, groups of saline (n= 12) or METH-treated animals (n=6 at 3d and n=12 at 30d) were sacrificed.

The brains were removed and divided sagitally. The left hemibrain was post-fixed in phosphate-buffered 4% paraformaldehyde (pH 7.4) at 4°C for 48 hr and sectioned at 40 μm with a Vibratome 2000 (Leica, Germany), while for the other hemibrain the caudate-putamen (striatum) was dissected for analysis of dopamine levels. Striatal tissue was assayed for DA content as described previously (Kuczenski et al., 1995; Schmidt et al., 1990). Briefly, tissue samples were weighed and homogenized by ultrasonication in 0.5 ml ice-cold 0.1M $HClO_4$ and centrifuged at 14,000 rpm for 15 min at 4°C. The supernatant was analyzed for DA content by HPLC-EC.

Neuropathology and analysis of neurodegeneration

Briefly, as previously described (Chana et al., 2003; Chana et al., 2006; Zhou et al., 2005), vibratome sections were stained with cresyl violet (1%) or immunostained with mouse monoclonal antibodies against NeuN (general neuronal marker, 1:1000, Chemicon International, Temecula, CA), calbindin (marker of interneurons, 1:1000, Sigma), dopamine transporter (DAT, 1:200, Chemicon), tyrosine hydroxylase (TH, 1:250, Chemicon), Iba-1 (microglial cell marker, 1:1000, DakoCytomation, Carpinteria, CA) or glial fibrillary acidic protein (GFAP, astroglial marker, 1:100, Chemicon), followed by biotinylated secondary antibodies, avidin coupled to horseradish peroxidase (HRP), and reacted with diaminobenzidine (DAB). Additional sections were immunostained with antibodies against microtubule-associated protein 2 (MAP2, dendritic marker, 1:20, Chemicon) and after overnight incubation, sections were incubated with fluorescein isothiocyanate (FITC)-conjugated horse anti-mouse IgG secondary antibody (1:75, Vector Laboratories, Burlingame, CA), transferred to SuperFrost slides (Fisher Scientific, Tustin, CA) and mounted under glass coverslips with anti-fading media (Vector). All sections were processed under the same standardized conditions. The immunolabeled blind-coded sections were serially imaged with the laser scanning confocal microscope (LSCM, MRC1024, BioRad, Hercules, CA) and analyzed with the Image 1.43 program (NIH), as previously described (Mucke et al., 1995; Toggas et al., 1994) to determine the percent area of the neuropil covered by MAP2-immunoreactive dendrites.

For stereological analysis of neuronal populations, briefly, sections stained with cresyl violet or immunostained with antibodies against NeuN, MAP2, calbindin, DAT and TH were analyzed with the optical disector as previously described (Chana et al., 2003; Zhou et al., 2006). Cells were sampled within a volume in the neocortex and hippocampus by optical

sectioning, at a 10 μm distance, within the vibratome section, using an Olympus BH2 microscope with a digital color camera attached to a DataCell computer assisted image analysis system (Image-Pro Plus, Media Cybernetics, Silver Spring, MD) for stereology. From each case at least 3 random sections within a given area of about 400 μm were analyzed and results were averaged and expressed as total number per cubic mm.

To evaluate the levels of immunoreactivity in the neuropil of selected brain regions, sections (3 per animal) immunostained with antibodies against DAT, TH, GFAP and Iba-1 were digitally imaged (groups of 10 digital images per section), and analyzed with Image-Pro Plus to determine optical density levels per field. Individual values were averaged and expressed as mean value.

Statistical analysis

All the analyses of each animal were conducted in triplicate on blind-coded samples. After the results were obtained, the code was broken and data were analyzed with the StatView program (SAS Institute, Inc., Cary, NC). Comparisons among the groups were performed by one-way ANOVA with post-hoc Dunnett's or Tukey-Kramer. All results were expressed as mean ±SEM.

Results

Degeneration of pyramidal neurons in the neocortex and hippocampus after METH binge

To investigate the patterns of neurodegeneration after the ED-MB treatment, neuropathological analysis was performed in cresyl violet-stained sections. Compared to saline-treated controls (Fig. 1A, D, G), at 3d after the last binge with METH, pyramidal neurons in the frontal cortex and the CA3 region of the hippocampus displayed mild shrinkage and disorganization that at 30d post last administration of METH became more severe (Fig. 1B, E, H). Stereological analysis showed that after 30d there was a significant 20 to 30% decrease in the number of pyramidal neurons in the neocortex (Fig. 1C) and in the CA3 region of the hippocampus with a wide range of variation (Fig. 1I). Overall, the neuronal changes were diffuse throughout the neocortical layers, although layers II and III were more affected. The total numbers of neurons in the dentate gyrus and CA1 region showed a trend toward a decrease, however the differences were not significant (Fig. 1F). To verify the alterations in neuronal numbers by an independent method, sections immunolabeled with the general neuronal marker NeuN were analyzed by stereology. This study showed that compared to saline-treated controls (Fig. 2A, D, G), 30d after the last administration of METH there was a significant 28% loss of pyramidal neurons in the fronto-parietal cortex (Fig. 2B, C) and an average 25% loss of neurons in the CA3 region of the hippocampus (Fig. 2E, H, I). While in some animals the loss was severe, amounting to up to 60%, in others the changes were more subtle (Fig. 2I).

To characterize in more detail the damage to pyramidal neurons, sections immunolabeled with an antibody against MAP2 were analyzed by confocal microscopy. Compared to saline-treated controls (Fig. 3A), in the neocortex of animals 30d after METH treatment, there was a widespread decrease of MAP2-immunoreactive neurons (Fig. 3B). Moreover, the remaining neurons displayed a considerable loss of their dendrite complexity 30d after the last administration of METH (Fig. 3B, C). Compared to saline-treated controls (Fig. 3D, G), in the hippocampus, a characteristic and well-demarcated zone within the CA3 region showed consistent loss of pyramidal neurons that ranged between 20 and 60% (Fig. 3E, H, I). Higher-power imaging demonstrated that compared to saline-treated controls (Fig. 4A, C, E), in METH-treated animals 30d after treatment, some pyramidal neurons also showed tortuous processes and dystrophic neurites consistent with neurodegeneration (Fig. 4) in the frontal cortex (Fig. 4B), and both the CA1 (Fig. 4F) and CA3 (Fig. 4D) regions of the hippocampus.

In contrast, no significant alterations in the levels of MAP2 immunoreactivity were observed in other brain regions such as the cerebellum.

The neurodegenerative alterations in the neocortex and hippocampus were accompanied by a trend toward increased astrogliosis, however these changes were not statistically significant (Table 2). In contrast, and compared to saline-treated controls (Fig. 5A, D, G), microglial cells displayed increased Iba-1 immunoreactivity and intense ramifications at 3d and more noticeably at 30d after METH treatment in the frontal cortex (Fig. 5B, C), hippocampus (Fig. 5E, F) and the CA3 region of the hippocampus (Fig. 5H, I).

Damage to calbindin interneurons in the brains of rats after METH binge treatment

Since previous studies have shown that interneurons are also susceptible to the neurotoxic effects of METH (Langford et al., 2003), we investigated the damage to this neuronal population in calbindin-immunostained sections. Compared to saline-treated controls (Fig. 6A), in layers 4–5 of the neocortex there was a 45% loss of calbindin-IR interneurons at both 3 and 30d after the last METH administration (Fig. 6B, C). There was a trend toward a mild decrease in the superficial layers of the neocortex at 30d. In the hippocampus there was a 40% decrease compared to controls in the numbers of calbindin-IR cells in the dentate gyrus (Fig. 6D–F) and a reduction in the levels of immunoreactivity of the neuropil in the CA3-CA2 region. In the basal ganglia there was a decrease in the levels of calbindin-IR in the neuropil at 3d after the last METH administration, with a partial recovery at 30d. The calbindin-IR neuronal population was relatively preserved (Fig. 6G–I).

To corroborate that the METH binge regimen resulted in dopaminergic deficits, analysis of DA levels by HPLC, and TH and DAT immunoreactivity by immunocytochemistry was performed. In agreement with our past results (Segal and Kuczenski, 1997; Segal et al., 2003), the ED-MB treatment resulted in a moderate 26% decrement in caudate-putamen dopamine levels when assessed 3d after the last METH injection; this decrement partially recovered to a 16% decrease by 30d (Table 2). Immunocytochemical analysis showed a 20% reduction in the density of TH and DAT-IR fibers in the neuropil of the caudate-putamen 3d after the last METH injection; however in the midbrain no significant differences in the density of TH positive neurons were detected (Table 2).

Discussion

The present study shows that, in addition to the well-known METH-induced disruption of striatal dopaminergic nerve terminals, prolonged METH exposure also results in extensive damage to pyramidal cells and interneurons in the neocortex and hippocampus. Importantly, persistent METH-induced alterations in cortical and hippocampal systems have also been documented in HIV+ patients with a history of METH abuse (Langford et al., 2003). Although no corroborating studies have been performed in non-HIV METH using individuals, our results in the rat model suggest a possible neuronal basis for METH-induced alterations.

This more extensive degeneration of pyramidal cells or interneurons is consistent with previous studies showing that METH promotes neuronal damage (O'Dell and Marshall, 2000) and apoptosis of neurons in several brain regions, including the neocortex, striatum and hippocampus (Deng et al., 2001). While previous studies used a single METH challenge or a series of five injections (5–10 mg/kg, every 2h), for the present study we used EDs for 14d with an 11-day binge starting on day 15. The ED treatment promotes tolerance to the sympathicomimetic and hyperthermic effects of METH and mimics some of the behavior of individuals who use METH. Accumulating evidence from a variety of approaches suggests that prolonged high-dose METH exposure results in persistent changes in cortical function. First, deficits in cognitive function following chronic exposure to METH have been attributed

to impairments in frontostriatal systems. These include, for example, impairments in abstraction and cognitive flexibility (Kalechstein et al., 2003; Lawton-Craddock et al., 2003; Sim et al., 2002; Simon et al., 2002), cognitive inhibition (Salo et al., 2002; Simon et al., 2002), working memory (Kalechstein et al., 2003; Rippeth et al., 2002), psychomotor processing speed (Kalechstein et al., 2003; Lawton-Craddock et al., 2003; Rippeth et al., 2002; Sim et al., 2002; Simon et al., 2002; Volkow et al., 2001a; Volkow et al., 2001c) and decision-making processes (Paulus et al., 2003). In addition, structural and functional changes in the cortex have been identified using a variety of imaging techniques. For example, Thompson et al used magnetic resonance imaging (MRI) to document METH-related decreases in the gray matter of the cingulate and other limbic cortices (Thompson et al., 2004). Chang and colleagues evaluated METH-dependent subjects using perfusion MRI and reported alterations in regional cerebral blood flow in parietal, temporoparietal and occipital brain regions (Chang et al., 2002). London et al characterized [^{18}F]fluorodeoxyglucose (FDG) positron emission tomography (PET) and found significant changes in the cingulate, insula and orbitofrontal areas (London et al., 2004). In addition, abnormal patterns of cortical metabolite levels have been detected by proton magnetic resonance spectroscopy (Nordahl et al., 2005; Nordahl et al., 2002). METH users had abnormally low NAA/Cr levels within the anterior cingulate cortex, consistent with neuronal loss. Furthermore, results of functional MRI (fMRI) during decision-making tasks suggest disruption of normal cortical function associated with METH use (Paulus et al., 2003; Paulus et al., 2002). Our findings of significant and substantial loss of pyramidal neurons in the frontal cortex support the contention that degeneration in the neocortex might underlie some of the long-term cognitive alterations in chronic METH users.

In addition to the selective loss of pyramidal neurons in the neocortex and limbic system, the animals in the present study displayed considerable damage to calbindin-IR interneurons in the neocortex and dentate gyrus of the hippocampus. In the neocortex, the calbindin-IR inhibitory cells are double bouquet interneurons that innervate sites near the distal dendrites of other neurons and are believed to play a role in regulating the firing rate of pyramidal excitatory neurons (Barbas et al., 2005) and modulating bi-directional neuronal responses that regulate cognitive responses such as working memory in the prefrontal cortex (Wang et al., 2004). Moreover, previous studies have shown that calbindin plays a major role in paired pulse facilitation (Blatow et al., 2003) and memory formation (Dumas et al., 2004). METH has been shown to suppress inhibitory neurons and disrupt the modulation of GABA-ergic synaptic transmission (Centonze et al., 2002). Moreover, METH has been shown to interfere with working memory in rats (Shoblock et al., 2003), however the selective effects of METH on calbindin-IR interneurons in experimental models has not yet been clearly defined. Nonetheless, studies in the neonatal rodent brain show that cocaine administration interferes with the migration and development of inhibitory neurons that could lead to serious deficits in cognitive performance (Crandall et al., 2004; Glezer et al., 1999). The preferential degeneration of these neurons after chronic METH use suggests that they become disconnected from bi-directional pathways that link prefrontal memory circuits.

The degeneration of calbindin-IR neurons demonstrated in the present study is consistent with our recent studies showing that in METH users with HIV encephalitis there is selective degeneration of this neuronal population that correlates with the patterns and severity of the cognitive alterations and memory loss in these patients (Langford et al., 2003). METH dependence has been shown to increase the risk for cognitive alterations in HIV patients (Rippeth et al., 2004). In addition, acceleration in the cognitive impairments of some HIV patients who use drugs may be due to destabilization of neuronal functioning by these drugs of abuse. However, although evidence in experimental animals also suggests that METH combined with HIV exposure may result in synergistic neurotoxicity (Maragos et al., 2002; Nath et al., 2001), our observations that prolonged exposure to METH alone results in

significant damage to calbindin-IR interneurons suggest that the stimulant may be primarily responsible for the degeneration of this neuronal population in METH users with HIV encephalitis. This possibility merits further investigation in METH users without a history of HIV.

The mechanisms through which chronic METH use might damage and promote degeneration of pyramidal neurons and calbindin-IR are not completely clear. Previous studies have suggested that METH promotes cell death by stimulating glutamate release, mitochondrial dysfunction, generating oxygen free radicals or reactive oxygen species, and disrupting calcium homeostasis (Bonavia et al., 2001; Flora et al., 2002; Koller et al., 2001; New et al., 1998). This might help explain the variability in the levels of injury to neurons in the CA3 region, since previous studies utilizing the excitotoxic glutamate analogue kainic acid show similar regional variability in neurotoxicity. It is possible that these regional differences in neuronal injury might be mediated by varying sensitivity of glutamate receptors among regions and in individual animals. However, it is important to note that in our model the loss of calbindin-IR interneurons became more apparent earlier (3d after the termination of the ED-MB) than the loss of pyramidal neurons. In the neocortex and hippocampus, at the earlier time point after the termination of the ED-MB treatment, there was retraction of the dendritic tree and collapse of the cell body of pyramidal neurons. This suggests that calbindin-IR cells might be more sensitive to METH toxicity than pyramidal neurons or that it takes longer for pyramidal cells to degenerate compared to interneurons. Moreover, these findings might indicate that in addition to the direct toxic effects of METH, other mechanisms leading to delayed degeneration of pyramidal neurons might be at play. In support of this possibility, we observed increased microglial activation in the neocortex and hippocampus suggesting that an inflammatory response mediated by the METH treatment might also participate in the degenerative process. Consistent with this possibility, studies have shown that METH treatment increases the expression of microglial markers such as Mac1 and isolectin-B4 (ILB4) in the striatum (Thomas et al., 2004) and attenuated microglial response results in tolerance to the neurotoxic effects of METH. METH has been shown to promote TNFα (Flora et al., 2002; Nakajima et al., 2004), interleukins 1α and 6 (IL1α, IL6) and monocyte chemoattractant protein (MCP) production by microglia that can be reduced by minocycline treatment (Sriram et al., 2006), some of which may contribute to the microglial activation observed in the present study.

In conclusion, these results support the notion that chronic METH use might promote more extensive and severe damage to selective neuronal populations than previously suspected, and the degeneration of these neuronal populations may be involved in the cognitive dysfunctions associated with high dose METH abuse.

Acknowledgments

This work was supported by NIH Grants MH59745, MH45294, MH58164, DA12065, DA01568, and DA02854, and a HNRC pilot project award. The HIV Neurobehavioral Research Center (HNRC) is supported by Center award MH 62512 from NIMH.

References

Barbas H, Medalla M, Alade O, Suski J, Zikopoulos B, Lera P. Relationship of Prefrontal Connections to Inhibitory Systems in Superior Temporal Areas in the Rhesus Monkey. Cereb Cortex. 2005

Blatow M, Caputi A, Burnashev N, Monyer H, Rozov A. Ca2+ buffer saturation underlies paired pulse facilitation in calbindin-D28k-containing terminals. Neuron 2003;38:79–88. [PubMed: 12691666]

Bonavia R, Bajetto A, Barbero S, Albini A, Noonan DM, Schettini G. HIV-1 Tat causes apoptotic death and calcium homeostasis alterations in rat neurons. Biochem Biophys Res Commun 2001;288:301–308. [PubMed: 11606043]

Centonze D, Picconi B, Baunez C, Borrelli E, Pisani A, Bernardi G, Calabresi P. Cocaine and amphetamine depress striatal GABAergic synaptic transmission through D2 dopamine receptors. Neuropsychopharmacology 2002;26:164–175. [PubMed: 11790512]

Chana G, Landau S, Beasley C, Everall IP, Cotter D. Two-dimensional assessment of cytoarchitecture in the anterior cingulate cortex in major depressive disorder, bipolar disorder, and schizophrenia: evidence for decreased neuronal somal size and increased neuronal density. Biol Psychiatry 2003;53:1086–1098. [PubMed: 12814860]

Chana G, Masliah E, Langford D, Adame A, Crews L, Grant I, Cherner M, Lazzaretto D, Heaton RK, Ellis RJ, Everall I. Cognitive deficits in HIV+ methamphetamine users is associated with loss of interneurons in the frontal cortex. Neurology. 2006 submitted.

Chang L, Ernst T, Speck O, Patel H, DeSilva M, Leonido-Yee M, Miller EN. Perfusion MRI and computerized cognitive test abnormalities in abstinent methamphetamine users. Psychiatry Res 2002;114:65–79. [PubMed: 12036507]

Crandall JE, Hackett HE, Tobet SA, Kosofsky BE, Bhide PG. Cocaine exposure decreases GABA neuron migration from the ganglionic eminence to the cerebral cortex in embryonic mice. Cereb Cortex 2004;14:665–675. [PubMed: 15054047]

Creese I, Iversen SD. The role of forebrain dopamine systems in amphetamine induced stereotyped behavior in the rat. Psychopharmacologia 1974;39:345–357. [PubMed: 4615333]

Deng X, Wang Y, Chou J, Cadet JL. Methamphetamine causes widespread apoptosis in the mouse brain: evidence from using an improved TUNEL histochemical method. Brain Res Mol Brain Res 2001;93:64–69. [PubMed: 11532339]

Dumas TC, Powers EC, Tarapore PE, Sapolsky RM. Overexpression of calbindin D(28k) in dentate gyrus granule cells alters mossy fiber presynaptic function and impairs hippocampal-dependent memory. Hippocampus 2004;14:701–709. [PubMed: 15318329]

Flora G, Lee YW, Nath A, Maragos W, Hennig B, Toborek M. Methamphetamine-induced TNF-alpha gene expression and activation of AP-1 in discrete regions of mouse brain: potential role of reactive oxygen intermediates and lipid peroxidation. Neuromolecular Med 2002;2:71–85. [PubMed: 12230306]

Glezer II, Toporovsky IM, Lima V, Yablonsky-Alter E. Cocaine adversely affects development of cortical embryonic neurons in vitro: immunocytochemical study of calcium-binding proteins. Brain Res 1999;815:389–399. [PubMed: 9878847]

Kalechstein AD, Newton TF, Green M. Methamphetamine dependence is associated with neurocognitive impairment in the initial phases of abstinence. J Neuropsychiatry Clin Neurosci 2003;15:215–220. [PubMed: 12724464]

Koller H, Schaal H, Freund M, Garrido SR, von Giesen HJ, Ott M, Rosenbaum C, Arendt G. HIV-1 protein Tat reduces the glutamate-induced intracellular Ca2+ increase in cultured cortical astrocytes. Eur J Neurosci 2001;14:1793–1799. [PubMed: 11860474]

Koob GF, Sanna PP, Bloom FE. Neuroscience of addiction. Neuron 1998;21:467–476. [PubMed: 9768834]

Kuczenski R, Segal DS, Cho AK, Melega W. Hippocampus norepinephrine, caudate dopamine and serotonin, and behavioral responses to the stereoisomers of amphetamine and methamphetamine. J Neurosci 1995;15:1308–1317. [PubMed: 7869099]

Langford D, Adame A, Grigorian A, Grant I, McCutchan JA, Ellis RJ, Marcotte TD, Masliah E. Patterns of selective neuronal damage in methamphetamine-user AIDS patients. J Acquir Immune Defic Syndr 2003;34:467–474. [PubMed: 14657756]

Lawton-Craddock A, Nixon SJ, Tivis R. Cognitive efficiency in stimulant abusers with and without alcohol dependence. Alcohol Clin Exp Res 2003;27:457–464. [PubMed: 12658111]

London ED, Simon SL, Berman SM, Mandelkern MA, Lichtman AM, Bramen J, Shinn AK, Miotto K, Learn J, Dong Y, Matochik JA, Kurian V, Newton T, Woods R, Rawson R, Ling W. Mood disturbances and regional cerebral metabolic abnormalities in recently abstinent methamphetamine abusers. Arch Gen Psychiatry 2004;61:73–84. [PubMed: 14706946]

Maragos WF, Young KL, Turchan JT, Guseva M, Pauly JR, Nath A, Cass WA. Human immunodeficiency virus-1 Tat protein and methamphetamine interact synergistically to impair striatal dopaminergic function. J Neurochem 2002;83:955–963. [PubMed: 12421368]

McCann UD, Wong DF, Yokoi F, Villemagne V, Dannals RF, Ricaurte GA. Reduced striatal dopamine transporter density in abstinent methamphetamine and methcathinone users: evidence from positron emission tomography studies with [11C]WIN-35, 428. J Neurosci 1998;18:8417–8422. [PubMed: 9763484]

Mucke L, Abraham C, Ruppe M, Rockenstein E, Toggas S, Alford M, Masliah E. Protection against HIV-1 gp120-induced brain damage by neuronal overexpression of human amyloid precursor protein (hAPP). J Exp Med 1995;181:1551–1556. [PubMed: 7699335]

Nakajima A, Yamada K, Nagai T, Uchiyama T, Miyamoto Y, Mamiya T, He J, Nitta A, Mizuno M, Tran MH, Seto A, Yoshimura M, Kitaichi K, Hasegawa T, Saito K, Yamada Y, Seishima M, Sekikawa K, Kim HC, Nabeshima T. Role of tumor necrosis factor-alpha in methamphetamine-induced drug dependence and neurotoxicity. J Neurosci 2004;24:2212–2225. [PubMed: 14999072]

Nath A, Maragos WF, Avison MJ, Schmitt FA, Berger JR. Acceleration of HIV dementia with methamphetamine and cocaine. J Neurovirol 2001;7:66–71. [PubMed: 11519485]

New DR, Maggirwar SB, Epstein LG, Dewhurst S, Gelbard HA. HIV-1 Tat induces neuronal death via tumor necrosis factor-alpha and activation of non-N-methyl-D-aspartate receptors by a NFkappaB-independent mechanism. J Biol Chem 1998;273:17852–17858. [PubMed: 9651389]

Nordahl TE, Salo R, Leamon M. Neuropsychological effects of chronic methamphetamine use on neurotransmitters and cognition: a review. J Neuropsychiatry Clin Neurosci 2003;15:317–325. [PubMed: 12928507]

Nordahl TE, Salo R, Natsuaki Y, Galloway GP, Waters C, Moore CD, Kile S, Buonocore MH. Methamphetamine users in sustained abstinence: a proton magnetic resonance spectroscopy study. Arch Gen Psychiatry 2005;62:444–452. [PubMed: 15809412]

Nordahl TE, Salo R, Possin K, Gibson DR, Flynn N, Leamon M, Galloway GP, Pfefferbaum A, Spielman DM, Adalsteinsson E, Sullivan EV. Low N-acetyl-aspartate and high choline in the anterior cingulum of recently abstinent methamphetamine-dependent subjects: a preliminary proton MRS study. Magnetic resonance spectroscopy. Psychiatry Res 2002;116:43–52. [PubMed: 12426033]

O'Dell SJ, Marshall JF. Repeated administration of methamphetamine damages cells in the somatosensory cortex: overlap with cytochrome oxidase-rich barrels. Synapse 2000;37:32–37. [PubMed: 10842349]

Paulus MP, Hozack N, Frank L, Brown GG, Schuckit MA. Decision making by methamphetamine-dependent subjects is associated with error-rate-independent decrease in prefrontal and parietal activation. Biol Psychiatry 2003;53:65–74. [PubMed: 12513946]

Paulus MP, Hozack NE, Zauscher BE, Frank L, Brown GG, Braff DL, Schuckit MA. Behavioral and functional neuroimaging evidence for prefrontal dysfunction in methamphetamine-dependent subjects. Neuropsychopharmacology 2002;26:53–63. [PubMed: 11751032]

Pu C, Broening HW, Vorhees CV. Effect of methamphetamine on glutamate-positive neurons in the adult and developing rat somatosensory cortex. Synapse 1996;23:328–334. [PubMed: 8855518]

Ricaurte GA, Guillery RW, Seiden LS, Schuster CR, Moore RY. Dopamine nerve terminal degeneration produced by high doses of methylamphetamine in the rat brain. Brain Res 1982;235:93–103. [PubMed: 6145488]

Ricaurte GA, Schuster CR, Seiden LS. Long-term effects of repeated methylamphetamine administration on dopamine and serotonin neurons in the rat brain: a regional study. Brain Res 1980;193:153–163. [PubMed: 7378814]

Ricaurte GA, Yuan J, Hatzidimitriou G, Cord BJ, McCann UD. Severe dopaminergic neurotoxicity in primates after a common recreational dose regimen of MDMA ("ecstasy"). Science 2002;297:2260–2263. [PubMed: 12351788]

Rippeth J, Heaton RK, Carey CL, Marcotte T, Moore DJ, Gonzalez R, Grant I. Effects of HIV infection and methamphetamine on specific cognitive domains. J Int Neuropsychol Soc 2002;8:188.

Rippeth JD, Heaton RK, Carey CL, Marcotte TD, Moore DJ, Gonzalez R, Wolfson T, Grant I. Methamphetamine dependence increases risk of neuropsychological impairment in HIV infected persons. J Int Neuropsychol Soc 2004;10:1–14. [PubMed: 14751002]

Salo R, Nordahl TE, Possin K, Leamon M, Gibson DR, Galloway GP, Flynn NM, Henik A, Pfefferbaum A, Sullivan EV. Preliminary evidence of reduced cognitive inhibition in methamphetamine-dependent individuals. Psychiatry Res 2002;111:65–74. [PubMed: 12140121]

Schmidt D, Roznoski M, Ebert MH. Qualitative and quantitative high performance liquid chromatographic analysis of monoamine neurotransmitters and metabolites in cerebrospinal fluid and brain tissue using reductive electrochemical detection. Biomed Chromatogr 1990;4:215–220. [PubMed: 1980626]

Schmued L, Bowyer J. Methamphetamiine exposure can produce neuronal degeneration in mouse hippocampal remnants. Brain Res 1997;759:135–140. [PubMed: 9219871]

Segal DS, Kuczenski R. An escalating dose “binge” model of amphetamine psychosis: behavioral and neurochemical characteristics. J Neurosci 1997;17:2551–2566. [PubMed: 9065515]

Segal DS, Kuczenski R, O’Neil ML, Melega WP, Cho AK. Escalating dose methamphetamine pretreatment alters the behavioral and neurochemical profiles associated with exposure to a high-dose methamphetamine binge. Neuropsychopharmacology 2003;28:1730–1740. [PubMed: 12865898]

Sekine Y, Iyo M, Ouchi Y, Matsunaga T, Tsukada H, Okada H, Yoshikawa E, Futatsubashi M, Takei N, Mori N. Methamphetamine-related psychiatric symptoms and reduced brain dopamine transporters studied with PET. Am J Psychiatry 2001;158:1206–1214. [PubMed: 11481152]

Shoblock JR, Maisonneuve IM, Glick SD. Differences between d-methamphetamine and d-amphetamine in rats: working memory, tolerance, and extinction. Psychopharmacology (Berl) 2003;170:150–156. [PubMed: 12774190]

Sim T, Simon SL, Domier CP, Richardson K, Rawson RA, Ling W. Cognitive deficits among methamphetamine users with attention deficit hyperactivity disorder symptomatology. J Addict Dis 2002;21:75–89. [PubMed: 11831502]

Simon SL, Domier CP, Sim T, Richardson K, Rawson RA, Ling W. Cognitive performance of current methamphetamine and cocaine abusers. J Addict Dis 2002;21:61–74. [PubMed: 11831501]

Sriram K, Miller DB, O’Callaghan JP. Minocycline attenuates microglial activation but fails to mitigate striatal dopaminergic neurotoxicity: role of tumor necrosis factor-alpha. J Neurochem 2006;96:706–718. [PubMed: 16405514]

Swerdlow NR, Vaccarino FJ, Amalric M, Koob GF. The neural substrates for the motor-activating properties of psychostimulants: a review of recent findings. Pharmacol Biochem Behav 1986;25:233–248. [PubMed: 2875470]

Thomas DM, Dowgiert J, Geddes TJ, Francescutti-Verbeem D, Liu X, Kuhn DM. Microglial activation is a pharmacologically specific marker for the neurotoxic amphetamines. Neurosci Lett 2004;367:349–354. [PubMed: 15337264]

Thompson PM, Hayashi KM, Simon SL, Geaga JA, Hong MS, Sui Y, Lee JY, Toga AW, Ling W, London ED. Structural abnormalities in the brains of human subjects who use methamphetamine. J Neurosci 2004;24:6028–6036. [PubMed: 15229250]

Toggas S, Masliah E, Rockenstein E, Mucke L. Central nervous system damage produced by expression of the HIV-1 coat protein gp120 in _transgenic mice. Nature 1994;367:188–193. [PubMed: 8114918]

Volkow ND, Chang L, Wang GJ, Fowler JS, Franceschi D, Sedler M, Gatley SJ, Miller E, Hitzemann R, Ding YS, Logan J. Loss of dopamine transporters in methamphetamine abusers recovers with protracted abstinence. J Neurosci 2001a;21:9414–9418. [PubMed: 11717374]

Volkow ND, Chang L, Wang GJ, Fowler JS, Franceschi D, Sedler MJ, Gatley SJ, Hitzemann R, Ding YS, Wong C, Logan J. Higher cortical and lower subcortical metabolism in detoxified methamphetamine abusers. Am J Psychiatry 2001b;158:383–389. [PubMed: 11229978]

Volkow ND, Chang L, Wang GJ, Fowler JS, Leonido-Yee M, Franceschi D, Sedler MJ, Gatley SJ, Hitzemann R, Ding YS, Logan J, Wong C, Miller EN. Association of dopamine transporter reduction with psychomotor impairment in methamphetamine abusers. Am J Psychiatry 2001c;158:377–382. [PubMed: 11229977]

Wang XJ, Tegner J, Constantinidis C, Goldman-Rakic PS. Division of labor among distinct subtypes of inhibitory neurons in a cortical microcircuit of working memory. Proc Natl Acad Sci U S A 2004;101:1368–1373. [PubMed: 14742867]

Wise RA, Rompre PP. Brain dopamine and reward. Annu Rev Psychol 1989;40:191–225. [PubMed: 2648975]

Zhou X, Long JM, Geyer MA, Masliah E, Kelsoe JR, Wynshaw-Boris A, Chien KR. Reduced expression of the Sp4 gene in mice causes deficits in sensorimotor gating and memory associated with hippocampal vacuolization. Mol Psychiatry 2005;10:393–406. [PubMed: 15558077]

Zhou X, Qyang Y, Kelsoe JR, Masliah E, Geyer MA. Impaired postnatal development of hippocampal dentate gyrus in Sp4 null mutant mice. Genes Brain Behav. 2006

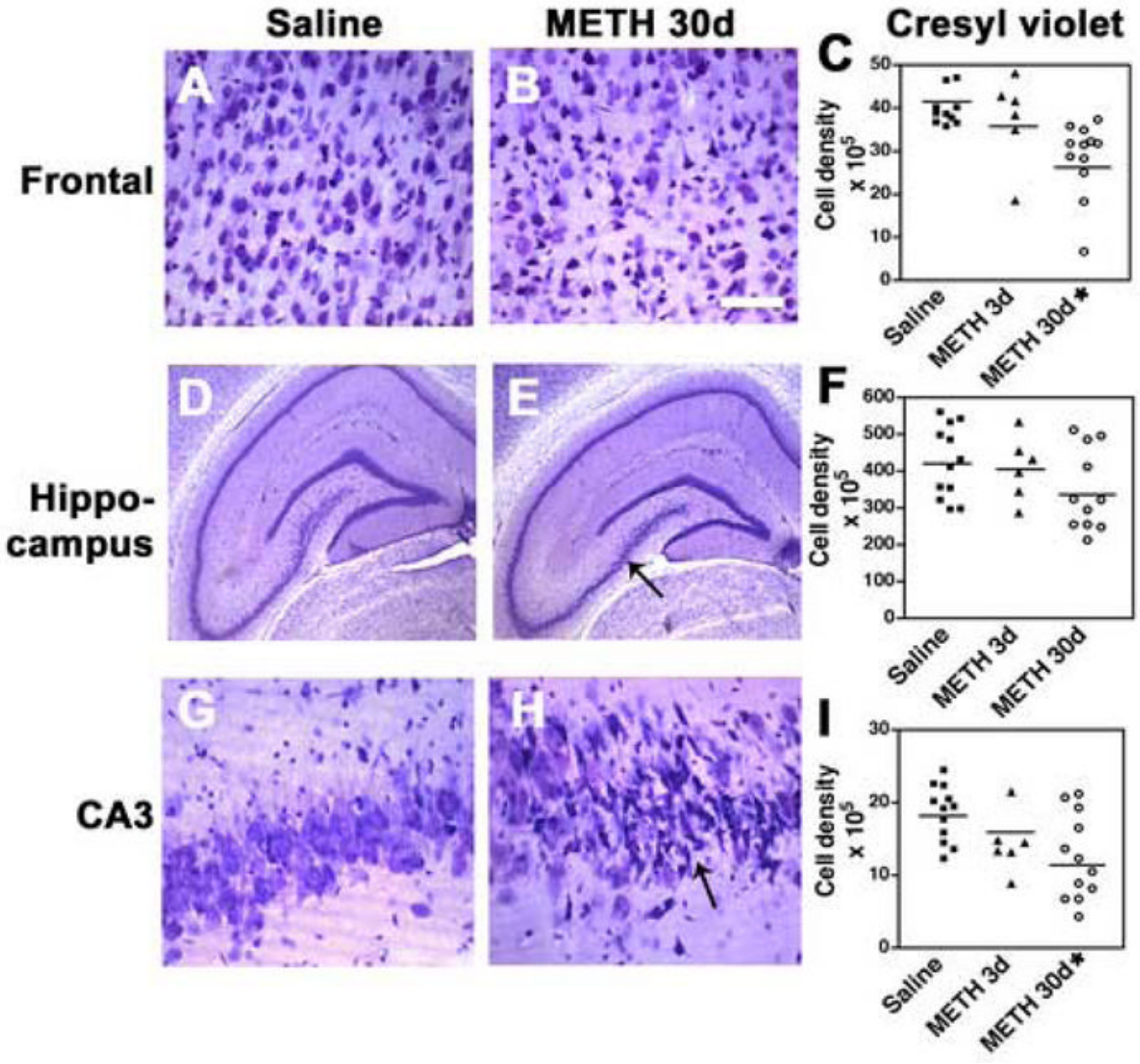

Fig. 1.

Neuronal density analysis after METH binge treatment in sections stained with cresyl violet. Neuronal counts were performed using the disector method with digitized images from the frontal cortex and hippocampus. (A) Representative image of the frontal cortex from a rat treated with saline showing the preservation of the patterns of neuronal lamination. (B) 30d post METH binge, frontal cortex pyramidal neurons in layers 2, 3 and 5 are shrunken and irregular. (C) Stereological analysis demonstrated a significant loss of neurons in the frontal cortex 30d after last binge. (D) Hippocampus from a rat treated with saline showing the preservation of the neuronal populations. (E) Hippocampal appearance in rats after 30d post METH binge showing alterations in pyramidal neurons in the CA3 region (arrow). (F) Stereological analysis demonstrated a trend toward reduced numbers of dentate granular neurons 30d after last binge. (G) CA3 hippocampal pyramidal neurons from a rat treated with saline. (H) After 30d post METH binge pyramidal neurons in CA3 are shrunken and irregular

(arrow). (I) Stereological analysis showing significant loss of CA3 neurons 30d after last binge. A, B scale bar, 50μM; D, E, scale bar, 1mM; G, H, scale bar, 30μM. *$p<0.05$ compared to saline-treated controls by one-way ANOVA with post hoc Dunnett's (n=12 saline-treated, n=6 at 3d and n=12 at 30d after last METH binge; note that some scatter plots may have overlapping points).

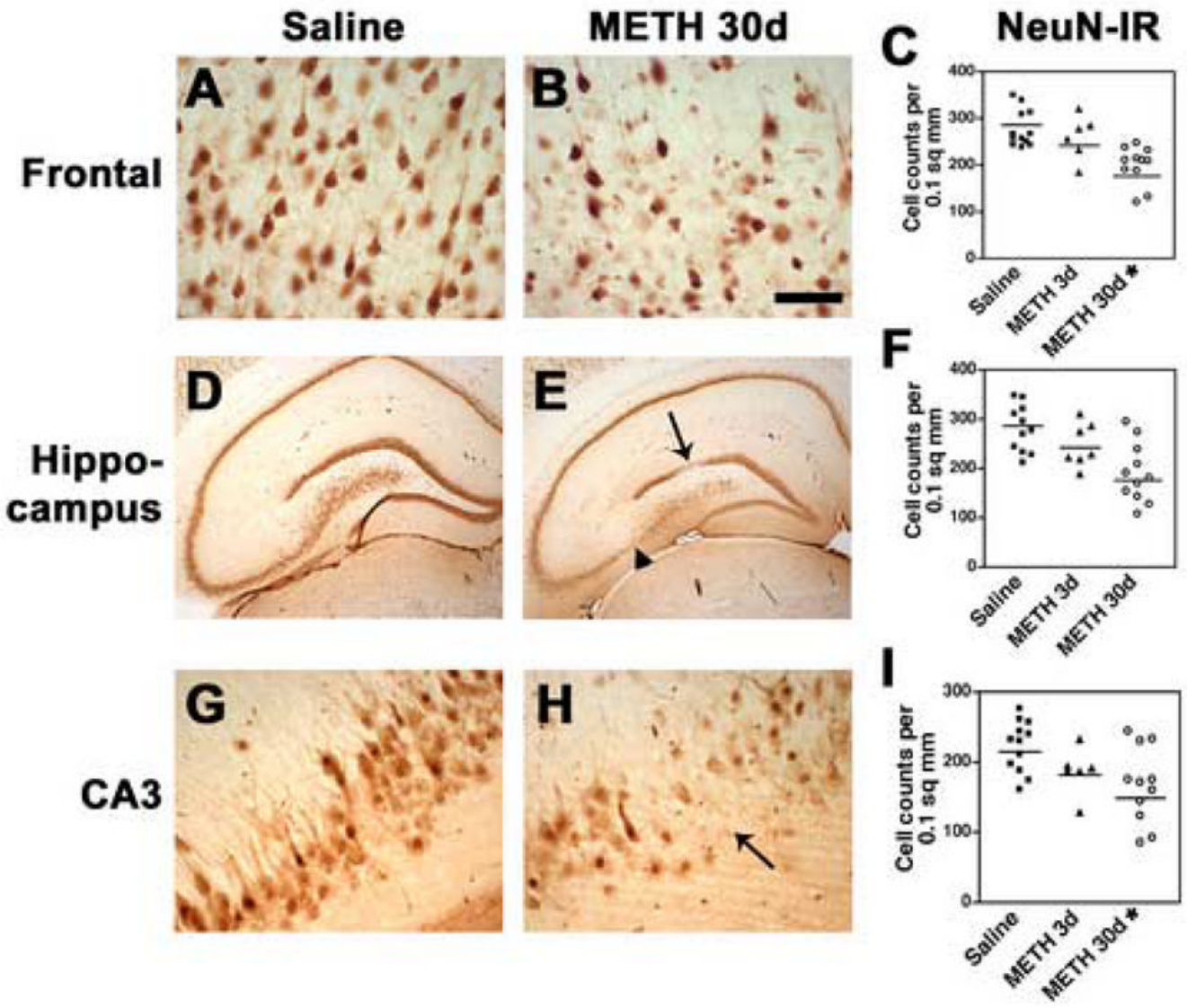

Fig. 2.

Alterations in the neocortex and hippocampus after METH binge treatment in sections immunostained with the neuronal marker, NeuN. Neuronal counts were performed using the disector method with digitized images from the frontal cortex and hippocampus. (A) Preservation of the neuronal populations in the frontal cortex of rats treated with saline. (B) 30d post METH binge there is reduction in the NeuN-immunostained pyramidal neurons in layers 2, 3 and 5. (C) Stereological analysis demonstrated a significant loss of NeuN-immunoreactivity (IR) in neurons of the frontal cortex 30d after the last binge. (D) Hippocampus from a rat treated with saline showing neuronal populations with normal characteristics. (E) Hippocampal appearance in rats after 30d post METH binge showing alterations in the dentate gyrus neurons (arrow) and CA3 pyramidal neurons (arrowhead). (F) Stereological analysis showing a trend towards reduced dentate granular neurons 30d after the last binge. (G) Pyramidal cells in the hippocampal CA3 region in rats treated with saline. (H) 30d post METH binge there is a reduction in NeuN-positive neurons in the CA3 region (arrow). (I) Stereological analysis showing significant loss of CA3 neurons 30d after the last binge. A, B scale bar, 50μM; D, E, scale bar, 1mM; G, H, scale bar, 50μM. *$p<0.05$ compared to saline-

treated controls by one-way ANOVA with post hoc Dunnett's (n=12 saline-treated, n=6 at 3d and n=12 at 30d after last METH binge; note that some scatter plots may have overlapping points).

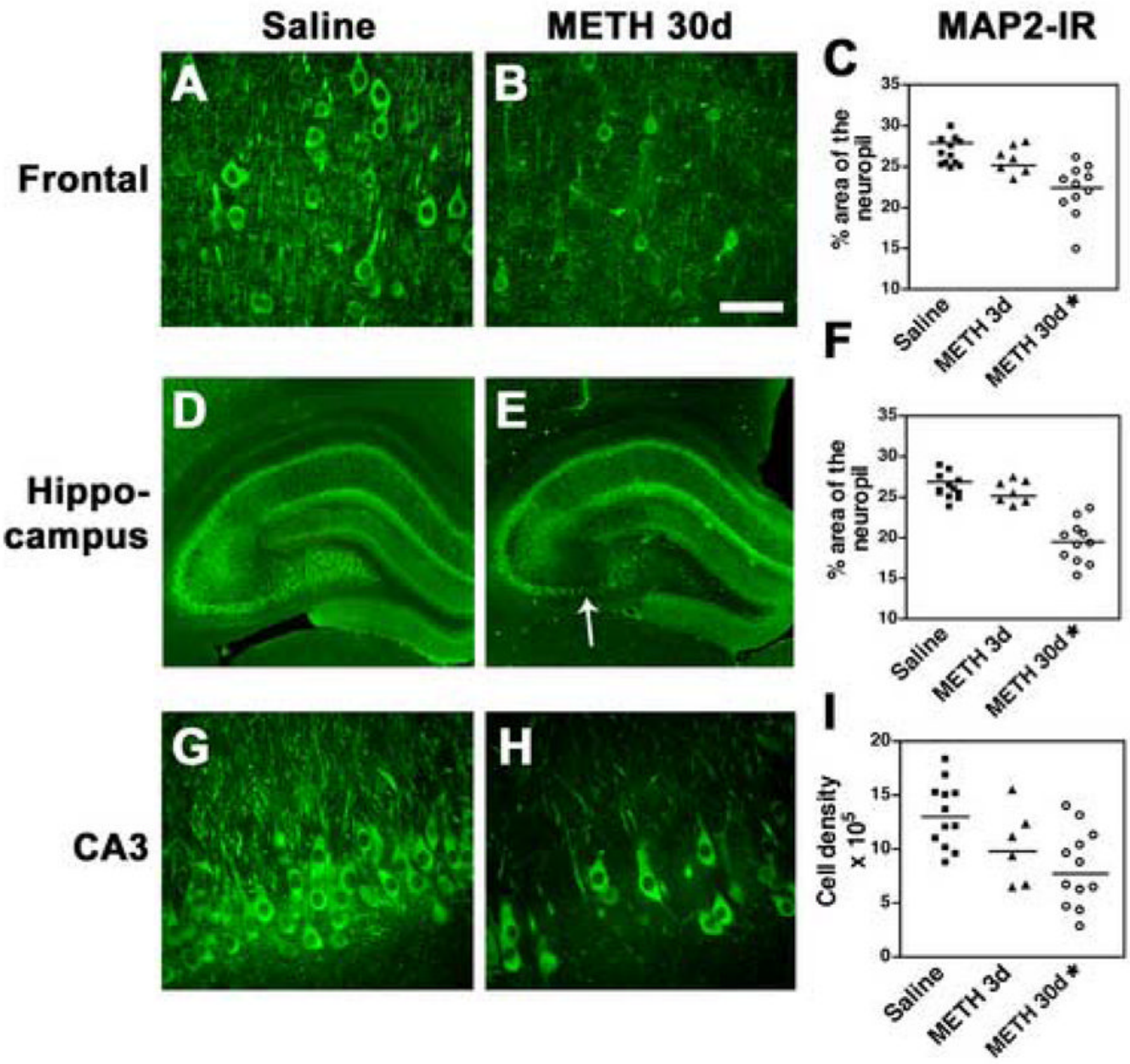

Fig. 3.

Alterations in MAP2 immunostaining in the neuropil after METH binge treatment. Sections were imaged with the laser scanning confocal microscope and the percent area of the neuropil was ascertained by image analysis. (A) In the frontal cortex of saline-treated rats, the neuronal populations and dendritic arbor display normal characteristics. (B) 30d post METH binge, the cell bodies and neuropil show reduced levels of MAP2 immunolabeling in the frontal cortex. (C) Stereological analysis demonstrated a significant decrease in MAP2-immunoreactivity (IR) 30d after the last binge. (D) The hippocampus from a saline-treated rat. (E) Hippocampal appearance in rats 30d post METH binge showing alterations in the dentate gyrus and CA3 region (arrow). (F) Stereological analysis showing a significant decrease in the levels of MAP2 immunostaining in the dentate gyrus 30d after the last binge. (G) Pyramidal cells in the hippocampal CA3 region in rats treated with saline. (H) 30d post METH binge there is a

reduction in MAP2 neurons in the CA3 region. (I) Stereological analysis showing significant loss of MAP2-IR CA3 neurons 30d after the last binge. A, B scale bar, 50μM; D, E, scale bar, 1mM; G, H, scale bar, 50μM. *$p<0.05$ compared to saline-treated controls by one-way ANOVA with post hoc Dunnett's (n=12 saline-treated, n=6 at 3d and n=12 at 30d after last METH binge; note that some scatter plots may have overlapping points).

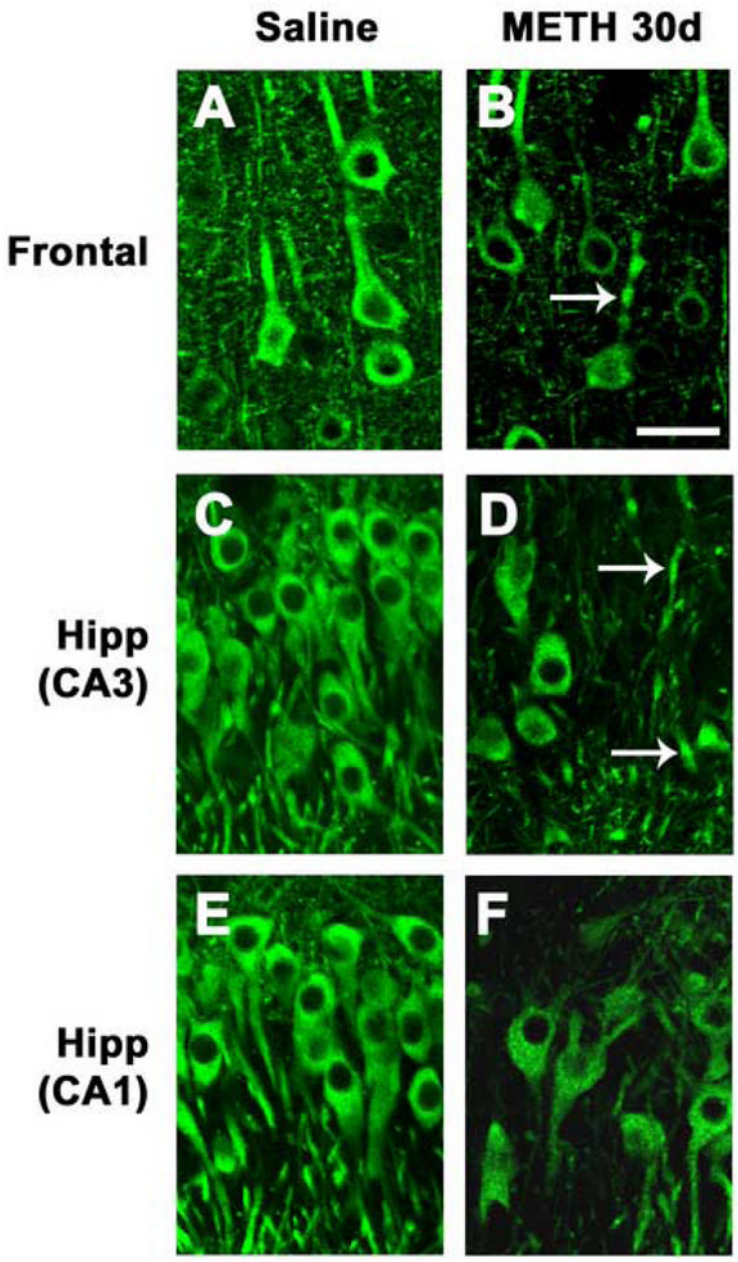

Fig. 4.

Dendritic pathology in the neocortex and hippocampus after METH binge treatment. Sections were immunolabeled with an antibody against MAP2 and imaged with the laser scanning confocal microscope. (A) Preserved dendritic architecture of frontal cortex neurons in a saline-treated rat. (B) 30d post METH binge, neurons in the frontal cortex are shrunken and some have dystrophic neurites (arrow). (C) Preserved dendritic architecture of neurons in the CA3 region of the hippocampus in a saline-treated rat. (D) 30d post METH binge, pyramidal CA3 neurons are shrunken with tortuous processes (arrows). (E) Preserved dendritic architecture of neurons in the CA1 region of the hippocampus in a saline-treated rat. (F) 30d post METH binge, pyramidal CA1 neurons are shrunken with tortuous processes. Scale bar, 20μM. *$p<0.05$ compared to saline-treated controls by one-way ANOVA with post hoc Dunnett's.

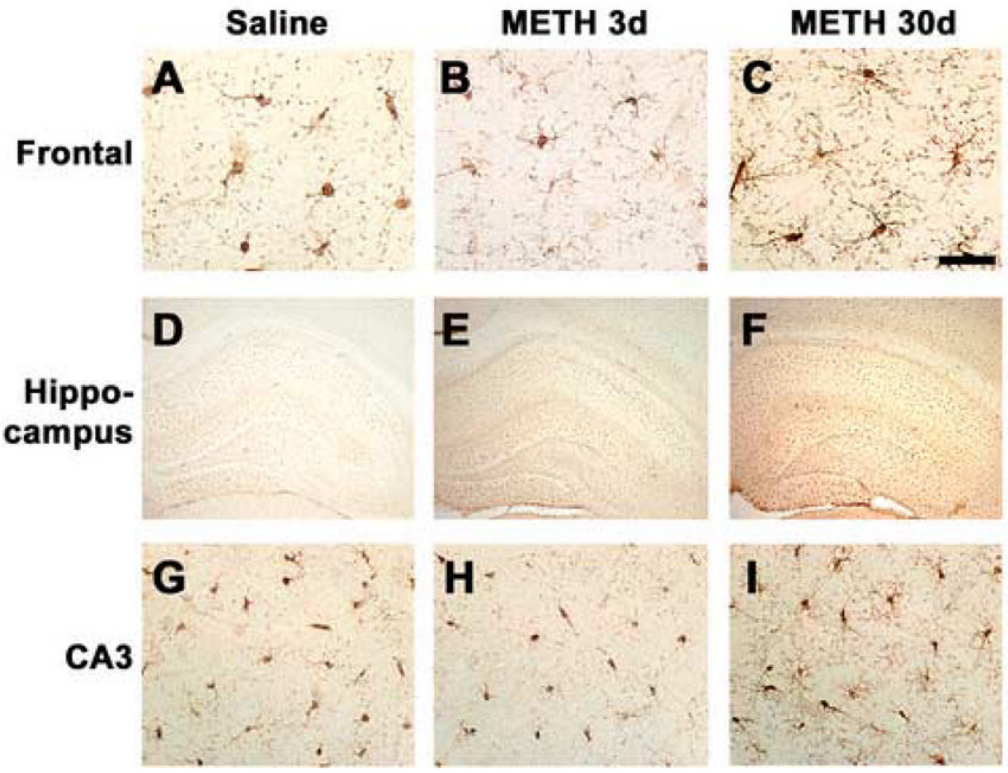

Fig. 5.

Microglial cell activation in the rat brain after METH binge treatment. Sections were labeled with an antibody against Iba-1 and imaged with bright field microscopy. (A–C) Activation of microglia in the frontal cortex after METH binge treatment. (D–F) Mild microglial cell activation in the hippocampus is detectable at 3d post METH binge, and is more prominent 30d post METH binge. (G–I) Activation of microglia in the CA3 region of the hippocampus after METH binge treatment. A–C, scale bar, 50μM; D–F, scale bar, 1mM; G–I, scale bar, 50μM.

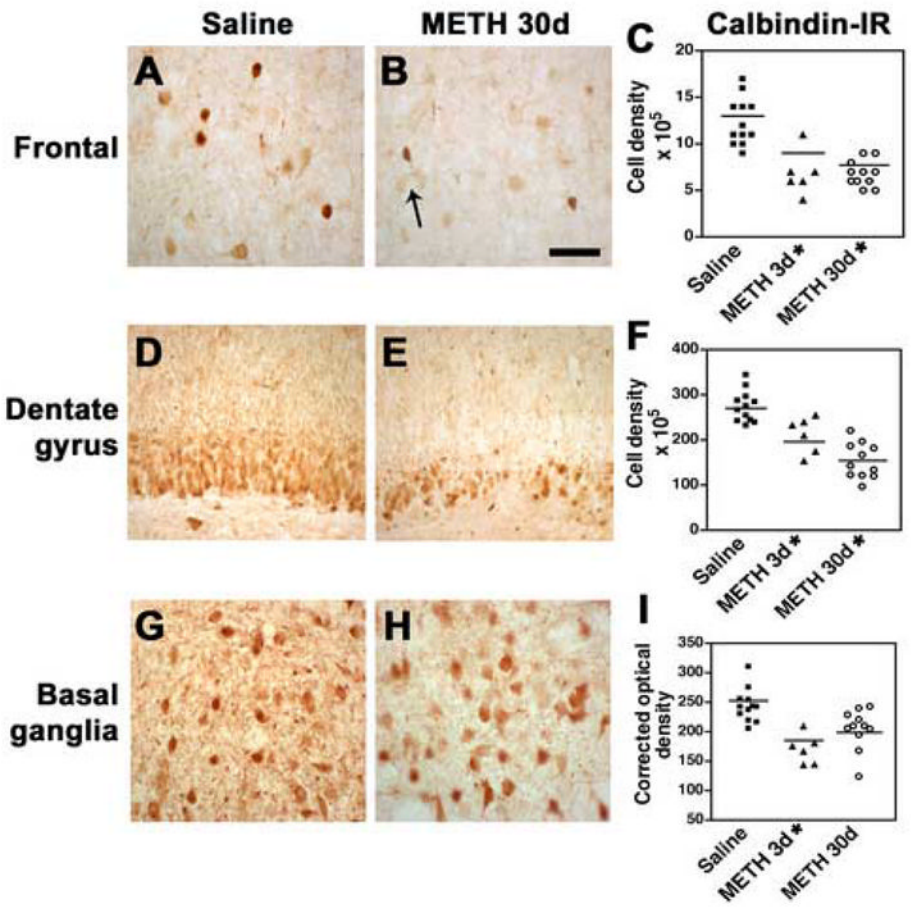

Fig. 6.

Damage to calbindin-immunoreactive interneurons in the rat after METH binge treatment. Calbindin-immunoreactive (IR) neuronal counts were performed using the disector method with digitized images from the frontal cortex, dentate gyrus and basal ganglia. (A) Preservation of the calbindin-IR interneuronal populations in the frontal cortex of rats treated with saline. (B) 30d post METH binge there is a trend towards a reduction in the calbindin-IR interneurons in the neocortex (arrow). (C) Stereological analysis demonstrated a significant loss of calbindin-IR in interneurons of the frontal cortex at 3d and 30d after the last binge. (D) Dentate gyrus from a rat treated with saline showing interneuronal populations with normal characteristics. (E) Dentate gyrus appearance in rats after 30d post METH binge showing decreased calbindin-immunoreactivity. (F) Stereological analysis showing significant loss of dentate granular calbindin-IR 30d after the last binge. (G) Normal calbindin-IR interneurons in the basal ganglia of a rat treated with saline. (H) 30d post METH binge there is a slight reduction in calbindin-IR in the dentate gyrus. (I) Stereological analysis showing significant loss of calbindin-IR interneurons at 3d and partial recovery at 30d after the last binge. A, B scale bar, 50μM; D, E, scale bar, 70μM; G, H, scale bar, 50μM. *$p<0.05$ compared to saline-treated controls by one-way ANOVA with post hoc Dunnett's.

Table 1

Escalating Dose Schedule of Administration

Day	Time		
	0900	1215	1630
	METH dose (mg/kg)		
Day 1	0.1	0.2	0.3
Day 2	0.4	0.5	0.6
Day 3	0.7	0.8	0.9
Day 4	1.0	1.1	1.2
Day 5	1.3	1.4	1.5
Day 6	1.6	1.7	1.8
Day 7	1.9	2	2.1
Day 8	2.2	2.3	2.4
Day 9	2.5	2.6	2.7
Day 10	2.8	2.9	3.0
Day 11	3.1	3.2	3.3
Day 12	3.4	3.5	3.6
Day 13	3.7	3.8	3.9
Day 14	4.0	4.0	4.0
Day 15–25	(4 × 6.0 mg/kg; 2h intervals)		

Table 2

Markers of astrogliosis and dopaminergic neuronal markers in the brains of METH-treated rats

Marker	Saline	METH 3d	METH 30d
Neocortex astrogliosis (GFAP-IR) optical density	175±17	221±28	228±23
Hippocampus astrogliosis (GFAP-IR) optical density	265±15	263±39	305±26
Caudo-putamen astrogliosis (GFAP-IR) optical density	144±10	192±18	232±15*
Caudo-putamen dopamine levels (p moles/g)	110.5±4.1	81.8±5.2*	90.6±4.3
Caudo-putamen DAT-IR neuropil (optical density)	256±11	175±16*	200±14
Midbrain DAT-IR neurons	6219±342	6014±514	5843±303
Caudo-putamen TH-IR neuropil (optical density)	276±10	205±22*	224±24
Midbrain TH-IR neurons	10,376±363	9322±506	9453±381

DAT = dopamine transporter; GFAP = glial acidic fibrillary protein; IR = immunoreactivity; TH = tyrosine hydroxylase

* $p<0.05$ compared to saline-treated controls by one-way ANOVA with post hoc Dunnett's